17th World Conference on Earthquake Engineering, 17WCEE
Sendai, Japan - September 27th to October 2nd 2021
Paper N° C000391
Registration Code: A-03089

PERFORMANCE OF SEISMICALLY ISOLATED LIQUID STORAGE TANKS USING TRIPLE PENDULUM BEARINGS

S.J. Ambrosio[(1)], E.J. Mamani[(2)] and V.I. Fernández-Dávila[(3)]

[(1)] *Research Assistant, Dept. Of Civil Engineering. National University of Engineering. Lima. Peru, sambrosioc@uni.pe*
[(2)] *Professor, Faculty of Engineering. Peruvian University of Applied Sciences. Lima. Peru. pccieman@upc.edu.pe*
[(3)] *Professor, Dept. Of Civil Engineering. National University of Engineering. Lima. Peru. vifdavila@uni.edu.pe*

Abstract

It presents the seismic response of circular cylindrical Reinforced Concrete (RC) liquid storage tanks which, besides playing a fundamental role in the water supply system, are also useful in the industry for the storage of petroleum, liquefied natural gas and chemical liquids, among others. In highly seismic countries such as Peru, it is very important that these structures remain operational after the occurrence of a severe seismic event. The most representative geometrical and dynamic parameters of the structural system were identified: ratio of water height and radius of the tank (H/R), effective period (T_{eff}), effective viscous damping (ζ_{eff}), and the level of seismic hazard considered (e.g. return period T_R). Subsequently, a family of 45 cases was generated from the combination of the four mentioned parameters to show the effectiveness of the triple friction pendulum bearings located at the base of the tanks. The regimes of displacement of the isolation system were configured to address specific response criteria for: SLE, Service Level Event (T_R = 72 years); DBE, Design Basis Event (T_R = 475 years); and MCE, Maximum Considered Event (T_R = 2,475 years). Time-history analyses were performed with 14 pairs of seismic records for different coefficients of friction, effective radii of the pendulum and displacement capacities of the isolators to study the effects of the parameters of the superstructure for different levels of seismic hazard. The main responses of interest were: the base shear, the overturning moment of the walls, the vertical displacement of the waves and the lateral displacement of the base of the tank; where a clear difference between the models was observed based on the effective period (3 and 4 seconds). In addition, it was appreciated that the parameter (H/R) was very influential in all the answers due to its direct relationship with the weight of the structure and its rigidity. The results show that the triple friction pendulum bearings have a good adaptability for different levels of seismic hazard and are effective to mitigate the seismic demand in tanks for liquid storage.

Keywords: triple pendulum bearing, RC liquid storage tanks, time-history analysis

1. Introduction

The seismic performance of liquid storage tanks is a matter of special importance, which extends beyond the economic value of the tank and its contents. Earthquakes can induce substantial hydrodynamic pressures on tank walls, and the overturning moment of the wall caused by lateral pressures could result in excessive compressive stresses on the bottom of one side of the tank and thus wall buckling of the tank avoiding its operation after the event [1].

Seismic isolation techniques have shown their effectiveness to improve seismic performance of liquid storage tanks [2, 3]. However, there is limited research on seismic responses of base-isolated tank-liquid systems using Triple Pendulum (TP) bearings [4]. It is a widespread practice to estimate seismic responses of fixed-base tank-liquid systems using Housner's equivalent mechanical model or one of its derivatives [3, 5, 6, and 7]. The main objective of this work is to contribute to the state-of-the-art knowledge of the seismic responses of RC liquid storage tanks using TP bearings subjected to bi-directional ground motions for multiple levels of seismic hazard (SLE, DBE and MCE) [8]. The specific objective of this work is to analyze the effects of parameters on the seismic responses.

2. Methodology

2.1 Structural model

Fixed-base and base-isolated tank-liquid structural models, were used to estimate the base shear, overturning moment of the wall, vertical sloshing displacement, and lateral displacement of the tank's base, where *H*, *R* and *t* are the liquid height, inner radius of the tank, and thickness of the wall, respectively (Figs. 1 and 2).

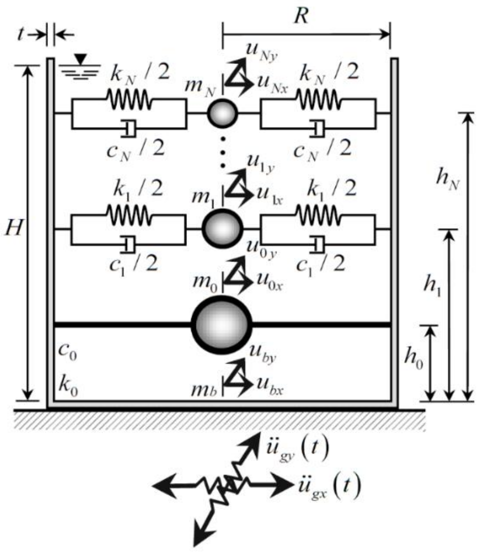

Fig. 1 – Fixed-base structural model

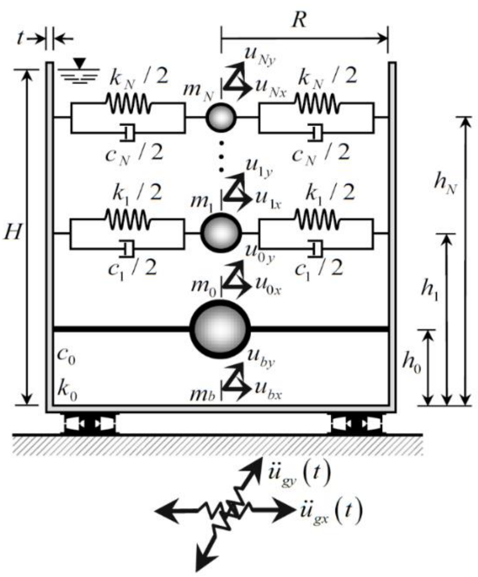

Fig. 2 – Base-isolated structural model

The total mass of liquid stored in the tank is represented by a series of concentrated masses producing equivalent forces and moments on the tank's walls due to horizontal ground motion during an earthquake, and the flexibility of the walls (Figs.1 and 2) was also considered. The portion of the liquid that participates in the open surface sloshing are called convective, where k_j, c_j, h_j and u_j are the stiffness, damping, height, and lateral displacement relative to the tank's base associated to the *j*th convective mass m_j. The portion of the liquid that moves jointly with the tank are called impulsive, where k_0, c_0, h_0 and u_0 are the stiffness, damping, height, and lateral displacement relative to the tank's base associated to the impulsive mass m_0. Furthermore, u_b is the lateral displacement of the tank's base relative to the ground, associated to the tank's net mass m_b; $\ddot{u}_g$ is the horizontal earthquake ground acceleration; and $m_l = m_0 + \sum^{\infty}_{j=1} m_j$ is the total mass of liquid. Finally, the total weight of the tank-liquid system can be expressed as $W = m_t\, g$, where $m_t = m_l + m_b$ is the total mass of the tank-liquid system and g is the gravitational acceleration. The following constants were considered: damping ratio ζ_l = 0.5% for the liquid and ζ_{RC} = 5% for the RC, modulus of elasticity E_{RC} = 21 300 MPa and Poisson's ratio ν_{RC} = 0.20 for the RC, density ρ_l = 1 000 kg/m^3 for the liquid and ρ_{RC} = 2 400 kg/m^3 for the RC. Special care was taken to represent the tank-liquid system with a wide range of convective modes of vibration (N), so that 90% or more of the participating mass could be included. Fig. 3, shows the accumulated percentage of modal participation factors, one can notice that over 99% of the hydrodynamic motion is sufficiently covered by the first three modes (N = 3) for H/R ratios larger than 0.5 [9].

2.2 Differential equations of motion

The differential equation describing the movement of the tank-liquid system (superstructure) is shown in Eq. (1). This equation assumes that the tank's base behaves as a rigid diaphragm in the plane supported by isolation system, and that the base of the isolation system is in direct contact with the foundation, where **M**, **C** y **K** are the diagonal mass, damping, and stiffness matrices of the superstructure; **l** is the earthquake's influence matrix.

$$\mathbf{M}\,\ddot{\mathbf{u}} + \mathbf{C}\,\dot{\mathbf{u}} + \mathbf{K}\,\mathbf{u} = -\mathbf{M}\,\mathbf{l}\,(\ddot{\mathbf{u}}_\mathbf{b} + \ddot{\mathbf{u}}_\mathbf{g}) \tag{1}$$

Furthermore, $\ddot{\mathbf{u}}$, $\dot{\mathbf{u}}$, and $\mathbf{u}$ represent the vectors of acceleration, velocity, and displacement associated to the degrees of freedom (Figs. 1 and 2) relative to the tank's base; $\ddot{\mathbf{u}}_\mathbf{b}$ is the acceleration vector of the tank's base relative to the ground; and $\ddot{\mathbf{u}}_\mathbf{g}$ is the ground acceleration vector. The differential equation describing the movement of the tank's base for the isolated system is shown in Eq. (2), where $\mathbf{M_b}$ is the diagonal mass matrix of the rigid tank's base.

$$\mathbf{l}^\mathbf{T}\,\mathbf{M}\,[\ddot{\mathbf{u}} + \mathbf{l}\,(\ddot{\mathbf{u}}_\mathbf{b} + \ddot{\mathbf{u}}_\mathbf{g})] + \mathbf{M_b}\,(\ddot{\mathbf{u}}_\mathbf{b} + \ddot{\mathbf{u}}_\mathbf{g}) + \mathbf{f} = \mathbf{0} \tag{2}$$

Furthermore, **f** is the vector containing the non-linear restoring forces of the isolation system [10].

2.3 Parametric cases

Two parameters were used to take into account the geometrical characteristics of the tank-liquid system: the ratio between the liquid height and the inner radius of the tank (H/R), and the ratio between the thickness of the tank's walls and the inner radius of the tank (t/R) [11]. Two parameters were used to take into account the geometrical and physical characteristics of the isolation system (Table 1): the effective period (T_{eff}), and the effective viscous damping (ζ_{eff}) [4]. Three parameters were used to take into account the level of seismic hazard: SLE, Service Level Event (T_R = 72 years); DBE, Design Basis Event (T_R = 475 years); and MCE, Maximum Considered Event (T_R = 2,475 years). The size of the internal radius of the tank remained constant throughout the study (R = 10 m).

Table 1 – Parameters used and the number of cases to be analyzed

ID	Tank-liquid		Triple pendulum (TP)		Seismic hazard level	Cases	
	H/R	t/R	T_{eff} (s)	ζ_{eff}	T_R (years)	Fixed-base	Base-isolated
1	0.5	0.04	3	0.10	72 (SLE)	9	36
2	1.0	---	4	0.25	475 (DBE)	---	---
3	2.0	---	---	---	2,475 (MCE)	---	---

(---) There is no value.

2.4 Earthquake ground motions

A set of 14 earthquake ground motions with moment magnitude, $M_w \geq 6.5$ were selected using QuakeManager [12]. The parameters considered in this research for selection are the same as those of the ASCE/SEI 07-16 standard procedures [13] and the escalation process is by amplitude.

For this research, a range of scale factors between 0.2 to 4 was used, it was scaled in the period range from 0.01 s to 7.00 s with uniform weight. The comparison spectrum for scaling was the natural logarithm of the displacement spectrum with a mean relative error of 0.25. A bi-directional RotD50 analysis [14] was performed for the three levels of seismic hazard (Fig. 3). The selected records are those listed in Table 2.

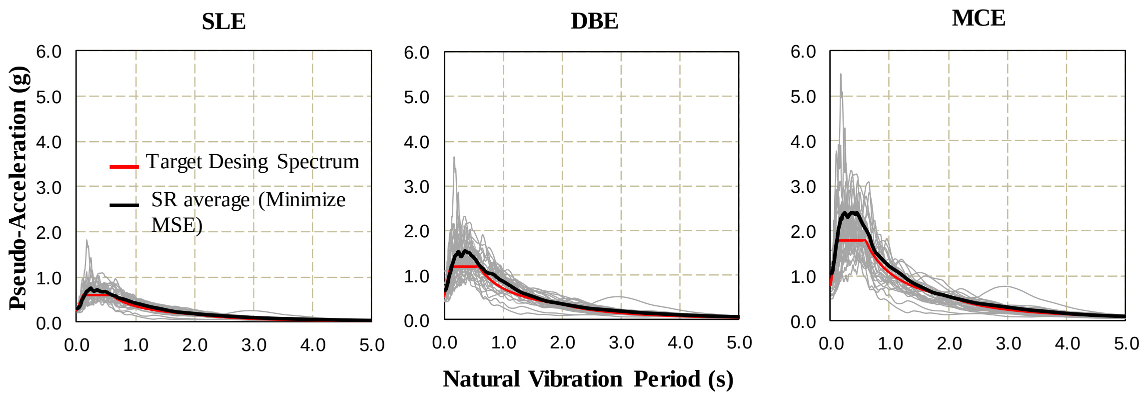

Fig. 3 – Amplitude scale average Spectrum Resultant (SR) to minimize Mean Squared Error (MSE) with respect to target design spectrum (5% damping ratio)

Table 2 – Selected earthquake ground motions and their scale factors

ID	Earthquake	Year	Station	Mw	SF SLE	SF DBE	SF MCE
1	Taiwan SMART1(45)	1986	Smart1 E01	7.3	1.23	2.43	3.66
2	Irpinia, Italy-01	1980	Calitri	6.9	1.57	3.15	4.00
3	Maule	2010	Angol V.1	8.8	0.51	1.02	1.53
4	Sur del Perú	2001	Arica Costanera V.2	8.4	1.15	2.29	3.44
5	Superstition Hills-02	1987	Kornbloom Road (temp)	6.5	1.74	3.48	4.00
6	Cape Mendocino	1992	Centerville Beach, Naval Fac	7.0	0.73	1.47	2.23
7	Northridge-01	1994	LA - Century City CC North	6.6	1.51	3.03	4.00
8	Maule	2010	Constitucion V.1	8.8	0.49	0.97	1.46
9	Pisco	2007	UNICA	8.0	0.69	1.38	2.07
10	Iwate	2008	IWT010	6.9	1.09	2.19	3.26
11	Hector Mine	1999	Joshua Tree	7.1	1.72	3.44	4.00
12	Sur del Perú	2001	César Vizcarra Vargas	8.4	1.13	2.26	3.39
13	Lima 1966	1966	Parque de la Reserva	8.1	1.29	2.58	3.87
14	Kobe	1995	Shin-Osaka	6.9	1.20	2.41	3.61

2.5 Simplified method of analysis

The simplified method evaluated here is that of effective stiffness and effective damping described in the standards and specifications for seismically isolated structures. The method is conceptually simple and uncomplicated. The method is based on the following steps: (a) represent the isolated structure by a single-degree-of-freedom system, (b) assume the peak isolator displacement, (c) construct the isolation system force–

displacement loop at the assumed displacement, (d) calculate the effective stiffness and effective damping on the basis of the constructed loop (the latter requires calculation of the energy enclosed by the hysteresis loop), (e) calculate the spectral displacement from the 5% damped response spectrum for the period corresponding to the effective stiffness, (f) calculate the displacement demand as the spectral displacement divided by the damping factor corresponding to the calculated effective damping, and (g) repeat the process of steps (b) to (f) until the assumed and calculated displacements are sufficiently close. Upon calculation of the displacement demand, the maximum isolation system force is obtained directly from the force–displacement loop [4].

Fig. 4 shows the geometry of a triple friction pendulum bearing. Its behavior is characterized by radii R_1, R_2, R_3 and R_4 (typically $R_1 = R_4$ and $R_2 = R_3$), heights h_1, h_2, h_3 and h_4, displacement capacities d_1, d_2, d_3 and d_4 (typically $d_2 = d_3$ and $d_1 = d_4$) and friction coefficients μ_1, μ_2, μ_3 and μ_4 (typically $\mu_2 = \mu_3$). Herein we consider that all isolators are of the same geometry and that the coefficients of friction represent the weighted average values for the entire isolation system [4]. The lateral force–displacement relation of the isolation system is illustrated in Fig. 5. Five different loops are shown in Fig. 5, each one valid in one of five different regimes of displacement.

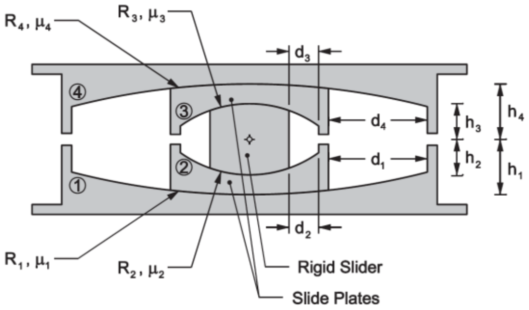

Fig. 4 – Cross section of the triple friction pendulum bearing [4].

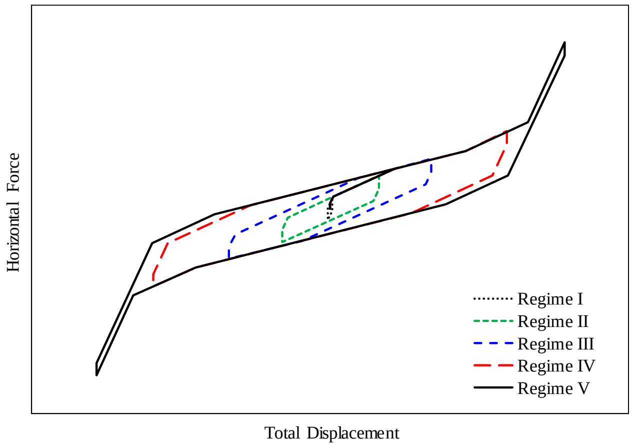

Fig. 5 – Force–displacement behavior of triple friction pendulum isolation system.

The effective stiffness (K_{eff}), effective period (T_{eff}), and effective damping (ζ_{eff}) are defined in Eq. 3, Eq. 4 and Eq. 5 respectively.

$$K_{eff} = F_{max}/D \tag{3}$$

$$T_{eff} = 2\pi[W/(gK_{eff})]^{1/2} \tag{4}$$

$$\zeta_{eff} = \mathrm{EDC}/(2\pi K_{eff} D^2) \tag{5}$$

Where F_{max} is the lateral force at displacement D and EDC is the energy dissipated in a cycle of harmonic motion at displacement amplitude D. Evaluation of EDC by analytical means is complex and it is best performed by first constructing the force–displacement relationship and then numerically evaluating the area enclosed by the loop [4].

2.6 Selected TP bearings

Four different geometric configurations were selected in terms of effective radii (to consider effective period), displacement capacities (to ensure that all possible regimes are activated) and coefficient of friction. Table 3 shows the geometric configuration (effective radii and displacement capacities) and Table 4 shows four different sets of friction coefficients.

Table 3 – Dimensions of triple friction pendulum bearings

Designation	Displacement capacities (mm)			Effective radii (mm)	
	$d_2 = d_3$	$d_1 = d_4$	d_{TOT}	$R_{eff2} = R_{eff3}$	$R_{eff1} = R_{eff4}$
3s - 10%	80	210	560	610	1,410
3s - 25%	70	180	480	3,00	2,200
4s - 10%	120	210	540	1,550	2,460
4s - 25%	70	165	430	1,000	3,950

Table 4 – Friction coefficient values

Designation	$\mu_2 = \mu_3$	μ_1	μ_4	$\mu_2 : \mu_1 : \mu_4$
3s - 10%	0.010	0.040	0.080	1 : 4 : 8
3s - 25%	0.020	0.060	0.100	1 : 3 : 5
4s - 10%	0.010	0.025	0.050	1 : 2.5 : 5
4s - 25%	0.015	0.040	0.060	1.5 : 4 :6

The effective period and effective damping of the TP bearings considered in the evaluation procedure are shown in Table 5. The effective radii are selected in such a way that the effective periods of the TP bearings in the third and fourth displacement regime occur during the most severe movements. Furthermore, the selection criteria of the coefficient of friction of the surfaces are based on the condition that a range of effective damping ratios can be provided for each geometric configuration.

Table 5 – Effective period and effective damping of TP bearings used

Configuration	Effective period (s)					Effective damping (%)				
	Displacement regime					Displacement regime				
	I	II	III	IV	V	I	II	III	IV	V
3s-10%	1.92	2.43	3.01	2.98	2.89	16	15	11	9	8
3s-25%	1.27	2.23	2.96	3.01	2.55	21	28	27	23	13
4s-10%	2.74	3.44	4.02	4.02	3.94	26	16	10	8	7
4s-25%	2.24	3.16	3.97	4.08	3.95	24	26	26	22	19

3. Analysis of the Results

In the present study, for bi-directional seismic excitation, the two components were applied simultaneously, where $\ddot{u}_{gx}$ and $\ddot{u}_{gy}$ are the earthquake accelerations in *x*- and *y*-directions, respectively (Figs. 1 and 2). The average value of the seismic responses obtained from the time-history analyses [15] was used to estimate the design seismic responses using the 14 selected and scaled pairs of ground motions [13].

3.1 Effect of TP beatings on seismic performance

Fig. 6 shows the seismic response in time for the fixed-base and base-isolated systems corresponding to one case study (H/R = 2.0, t/R = 0.04, T_{eff} = 4s, ζ_{eff} = 25% and T_R = 2,475 years) subjected to scaled ground motion from the Pisco 2007 earthquake.

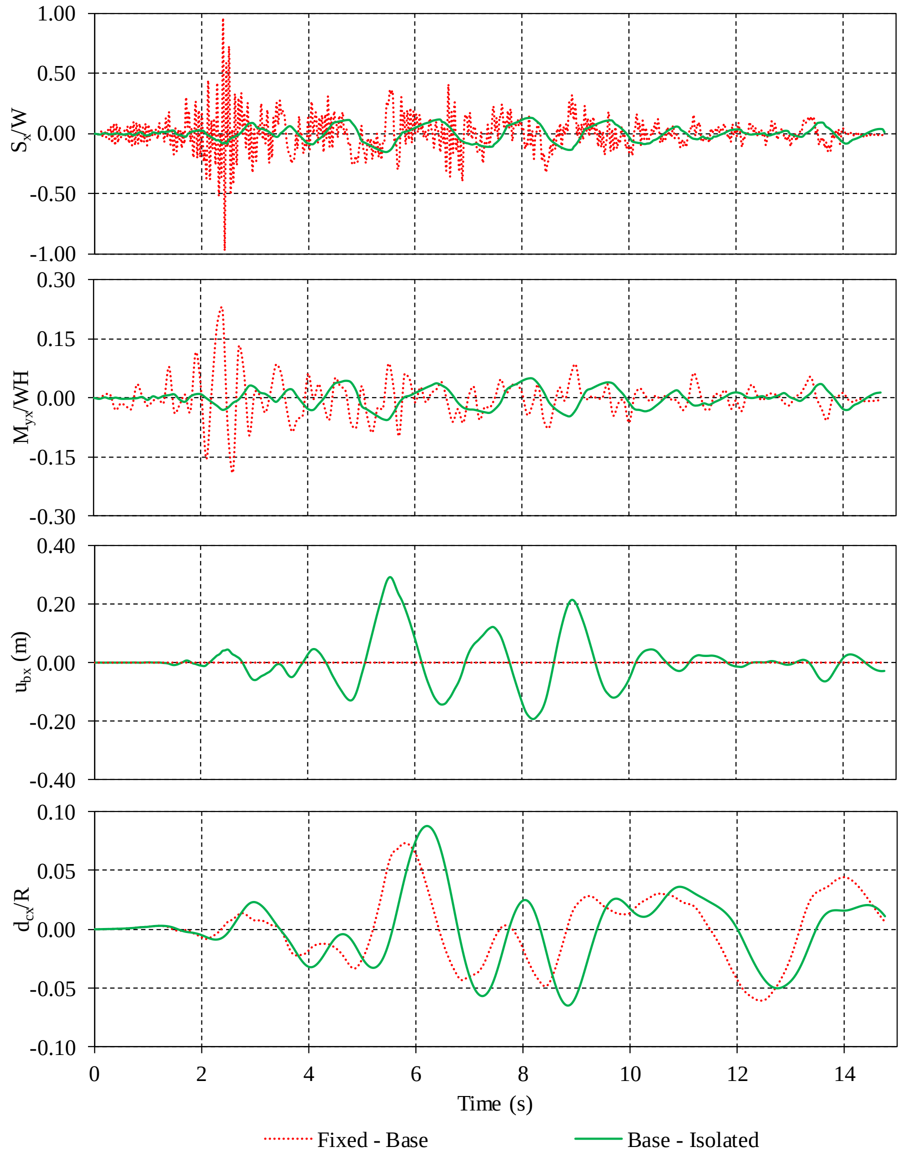

Fig. 6 – Seismic responses in time for fixed-base and base-isolated systems (H/R = 2.0, t/R = 0.04, T_{eff} = 4s, ζ_{eff} = 25% and T_R = 2,475 years) due to Pisco 2007 earthquake (scaled ground motion)

Where S_x is the base shear in the x-direction, M_{yx} is the overturning moment of the walls in the y-direction due to forces in the x-direction, u_{bx} is the lateral displacement of the tank's base relative to the ground in the x-direction and u_{jx} is the lateral displacement of m_j relative to the tank's base in the x-direction. Furthermore, $d_{cx} = \sum_{j=1}^{\infty} u_{jx}\, \lambda_j\, \varepsilon_j \tanh(\lambda_j\, H/R)$ is the vertical sloshing displacement of the free water surface in contact with the tank's walls along the x-direction, where $\varepsilon_j = 2/(\lambda^2_j - 1)$, λ_j is the jth root of $J'_1(\lambda) = 0$ and J_1 is the Bessel function of the first kind of the first order [3].

It can be appreciated that the isolation system effectively reduced the maximum base shear, the maximum overturning moment of the walls compared to the fixed base system. On the other hand, the convective period must be taken into account when the effective period and effective damping are selected for avoid an increase of the vertical sloshing displacement.

As shown in Fig. 7, there is good agreement between the force-displacement loops obtained from the time-history analysis and the theoretical hysteresis loop. Therefore, the results of the numerical model can be used to predict the responses of the superstructure and TP bearings.

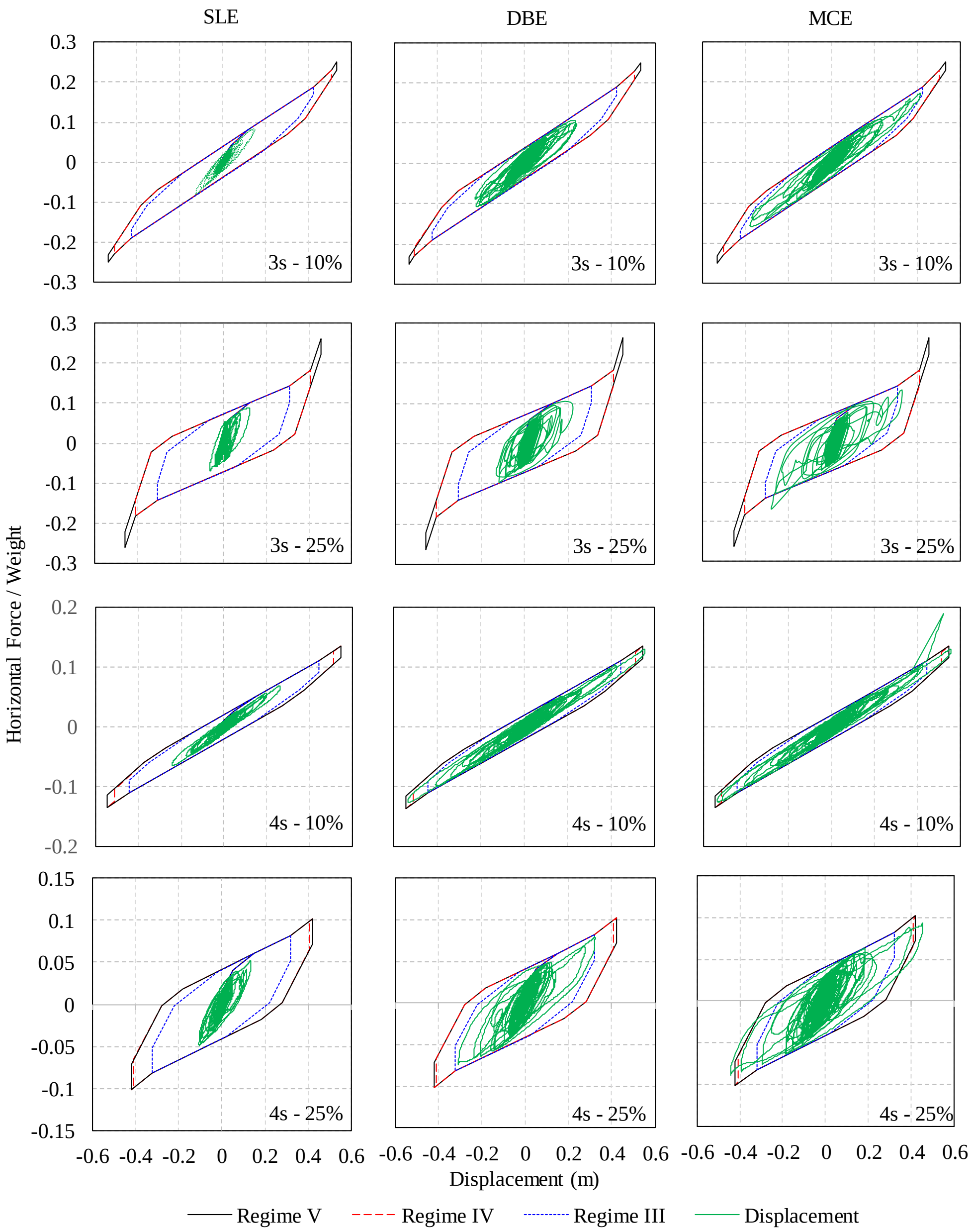

Fig. 7 – Force-displacement loops of base-isolated system (H/R = 2.0 and t/R = 0.04) due to Pisco 2007 earthquake (scaled ground motion)

3.2 Effects of study parameters

Fig. 8 shows the normalized design seismic responses in the *x*-direction, corresponding to fixed base systems and base-isolated systems, with T_{eff} of 3s and 4s, and ζ_{eff} of 10% and 25%, under bi-directional seismic excitation due to the three levels of seismic hazard considered (SLE, DBE and MCE), results in the following observations:

a) The reduction in base shear when compared to the fixed-base system is 36% to 67% for *H*/*R* = 0.5; 59% to 81% for *H*/*R* = 1.0; and 78% to 90% for *H*/*R* = 2.0.

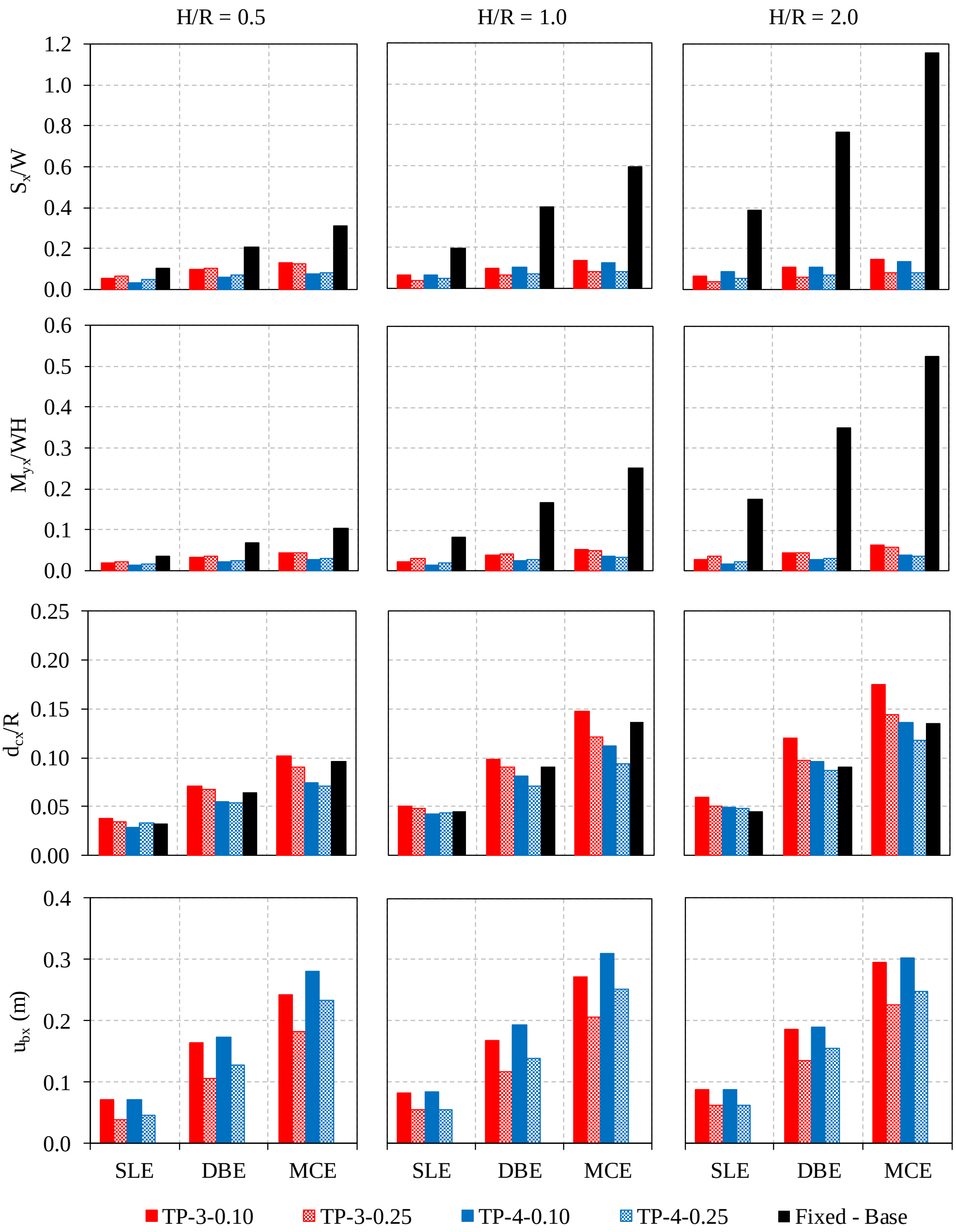

Fig. 8 – Effect of parameters T_{eff} and ζ_{eff} on normalized design seismic responses of base-isolated systems (*H*/*R* = 0.5, 1.0 and 2.0; *t*/*R* = 0.04; SLE, DBE and MCE) and comparison to fixed-base systems.

b) The reduction in overturning moment of the walls when compared to the fixed-base system is 39% to 64% for H/R = 0.5; 63% to 86% for H/R = 1.0; and 80% to 92% for H/R = 2.0.
c) The variation in vertical sloshing displacement when compared to the fixed-base system is −17% to 27% for H/R = 0.5; −12% to 31% for H/R = 1.0; and −31% to 13% for H/R = 2.0.
d) For H/R = 0.5 is more effective T_{eff} = 4s and ζ_{eff} = 10% and for H/R = 1.0 and H/R = 2.0 is more effective T_{eff} = 3s and ζ_{eff} = 25% in the reduction of the base shear.
e) For H/R = 0.5, H/R = 1.0 and H/R = 2.0 is more effective T_{eff} = 4s and ζ_{eff} = 10% in the reduction of the overturning moment of the walls.
f) For H/R = 0.5, H/R = 1.0 and H/R = 2.0 is more effective T_{eff} = 4s and ζ_{eff} = 25% in the reduction of the vertical sloshing displacement.
g) The lateral displacement of the tank's base relative to the ground increase through the three levels of seismic hazard (from SLE to DBE and from DBE to MCE), this increase is more for T_{eff} = 3s and ζ_{eff} = 10% and T_{eff} = 4s and ζ_{eff} = 10%.

4. Conclusions

The following conclusions of the investigation are valid for the group of defined parametric cases, corresponding to tanks with a TP type insulation system.

1. The TP bearings are effective in the reduction of the base shear force and the overturning moment of the walls with respect to fixed base systems for all levels of seismic hazard analyzed.
2. The TP bearings are more effective for H/R = 1.0 and H/R = 2.0 than for H/R = 0.5.
3. The parameters that reduce all the seismic responses at the same time are T_{eff} = 4s and ζ_{eff} = 25%.
4. The simplified method evaluated here is conceptually simple and uncomplicated.

5. Acknowledgements

The authors wish to express their gratitude to the Department of Civil Engineering of the National University of Engineering of Peru and the Faculty of Engineering of the Peruvian University of Applied Sciences.

6. References

[1] Zareian F, Aguirre C, Beltrán JF, Cruz E, Herrera R, Leon R, Millan A, Verdugo A (2012): Reconnaissance report of Chilean industrial facilities affected by the 2010 Chile offshore Bío-Bío earthquake. *Earthquake Spectra*, **28** (S1), S513–S532.

[2] Malhotra PK (1997): New methods for seismic isolation of liquid-storage tanks. *Earthquake Engineering and Structural Dynamics*, **26** (8), 839–847.

[3] Wang YP, Teng MC, Chung, KW (2001): Seismic isolation of rigid cylindrical tanks using friction pendulum bearings. *Earthquake Engineering and Structural Dynamics*, **30** (7), 1083-1099.

[4] Fadi F., Constantinou MC (2010): Evaluation of simplified methods of analysis for structures with triple friction pendulum isolators. *Earthquake Engineering and Structural Dynamics*, **39** (1), 5-22.

[5] Housner GW (1957): Dynamic pressures on accelerated fluid containers. *Bulletin of Seismological Society of America*, **47** (1), 15–35.

[6] Haroun MA, Housner GW (1981): Seismic design of liquid storage tanks. *Journal of Technical Councils of ASCE*, **107** (1), 191–207.

[7] Veletsos AS (1984): Seismic response and design of liquid storage tanks. Guidelines for the seismic design of oil and gas pipeline systems. *Technical Council on Lifeline Earthquake Engineering* 255-370, 443-461, ASCE, New York, USA.

[8] Morgan TA, Mahin SA (2010): Achieving reliable seismic performance enhancement using multi-stage friction pendulum isolators. *Earthquake Engineering and Structural Dynamics*, **39** (13), 1443-1461.

[9] Mamani EJ (2017). *Respuesta sísmica de tanques de concreto armado para aislamiento de agua apoyados sobre un sistema de aislamiento del tipo péndulo friccional*. Pontifical Catholic University of Peru, Lima, Perú.

[10] Nagarajaiah S, Reinhorn AM, Constantinou MC (1991): Nonlinear dynamic analysis of three-dimensional base isolated structures. *Journal of Structural Engineering, ASCE*, **117** (7), 2035-2054.

[11] Priestley MJN, Wood JH, Davidson BJ (1986): Seismic design of storage tanks. *Bulletin of the New Zealand National Society for Earthquake Engineering*, **19** (4), 272-284.

[12] Hachem MM (2008): QuakeManager: A software framework for ground motion record management, selection, analysis and modification. *14th World Conference on Earthquake Engineering WCEE*, Beijing, China.

[13] ASCE/SEI 7 (2016): *Minimum design loads for buildings and other structures*. American Society of Civil Engineers, Virginia, USA.

[14] Boore, DM (2010). Orientation-independent, nongeometric-mean measures of seismic intensity from two horizontal components of motion. Bulletin of the Seismological Society of America. **100** (4), 1830-1835.

[15] CSI (2014): *SAP2000 v17*. Computers and Structures Incorporated, Berkeley, USA.